The influence of Gd on magnetic and electric transport properties in $La_{0.67-x}Gd_xSr_{0.33}CoO_3$

2004 J. Phys.: Condens. Matter 16 103

(http://iopscience.iop.org/0953-8984/16/1/010)

INSTITUTE OF PHYSICS PUBLISHING JOURNAL OF PHYSICS: CONDENSED MATTER

J. Phys.: Condens. Matter **16** (2004) 103–115 PII: S0953-8984(04)67144-X

The influence of Gd on magnetic and electric transport properties in $La_{0.67-x}Gd_xSr_{0.33}CoO_3$

Wei Tong, Liangbing Hu, Hong Zhu, Shun Tan and Yuheng Zhang

Structure Research Laboratory, University of Science and Technology of China, Hefei 230026, People's Republic of China
and
National High Field Laboratory, Hefei 230031, People's Republic of China

E-mail: zhangyh@ustc.edu.cn

Received 5 August 2003
Published 15 December 2003
Online at stacks.iop.org/JPhysCM/16/103 (DOI: 10.1088/0953-8984/16/1/010)

Abstract

The magnetic and transport properties of the polycrystalline samples $La_{0.67-x}Gd_xSr_{0.33}CoO_3$ ($0 \leqslant x \leqslant 0.67$) are investigated. On incorporation of Gd, the Curie temperature T_C progressively shifts to lower temperature, and the magnetization increases rapidly below 60 K with decreasing temperature. This increase of magnetization can be attributed to the paramagnetism of the Gd sublattice. However, in the system $La_{0.7-x}Gd_xSr_{0.3}MnO_3$ the Gd sublattice forms a ferromagnetic structure at high-doping level, and the magnetic moments of the Gd sublattice are antiparallel to those of the Mn sublattice. The resistivity curves show a metal–semiconductor transition upon doping with Gd, and $x = 0.40$ is the critical doping point. The experimental resistivity can be fitted by the expression $\rho = \rho_0 + \rho_2 T^2$ for metallic samples below T_C. In the metallic samples ($x < 0.4$) the magnetoresistance (MR) peak is near the Curie temperature, and the MR occurs over a large temperature range. With decreasing temperature, the peak is reduced and the MR range is narrowed. For insulating compositions ($x > 0.4$) the MR peak near T_C disappears and the low-temperature MR is greatly enhanced.

1. Introduction

Since Von Helmolt *et al* first reported the colossal magnetoresistance (CMR) discovered in LaBaMnO film in 1993, [1] this type of perovskite oxide has received extensive and intensive studies [2]. So far, the double-exchange (DE) theory suggested by Zener, and the Jahn–Teller (JT) effect associated with Mn^{3+} ions have become two key roles for understanding the conductive mechanism of the mixed-valence manganites $La_{1-x}M_xMnO_3$ (M = Ca, Sr, Ba, Pb, etc) [3].

During this period, Briceño *et al* [4] discovered large magnetoresistance in another type of perovskite compound, $La_{1-x}M_xCoO_3$ (M = Ba, Sr, Ca, Pb) in 1995. However, unlike Mn-based oxides to which the most of the attention has been paid, there are very few reports on

the magnetoresistance of Co-based oxides, and most of the recent studies have concentrated only on $La_{1-x}Sr_xCoO_3$ and $LaCoO_3$ [5–10].

The differences between Mn-based oxides and Co-based oxides can basically be attributed to the characteristic electronic structure and spin configuration of Mn and Co ions. In the parent compound $LaMnO_3$, the spin configuration of Mn^{3+} is $t_{2g}^3e_g^1$ with $S = 2$. The substitution of divalent alkaline-earth elements for La in $LaMnO_3$ leads to the conversion of Mn^{3+} into Mn^{4+} ions which are in the $t_{2g}^3e_g^0$ state ($S = 3/2$). Their spin states are invariable with temperature in Mn-based perovskite because the Hund's rule coupling of the carrier (e_g electron) to the core spin (t_{2g} electrons) is larger than the crystal field energy. Yet in Co-based perovskite the situation is complicated. In $LaCoO_3$, trivalent Co ions are all in the low-spin (LS) state Co^{III} ($t_{2g}^6e_g^0$, $S = 0$) at the lowest temperature. With increasing temperature (35–110 K), Co^{III} is progressively converted into the high-spin (HS) state Co^{3+} ($t_{2g}^4e_g^2$, $S = 2$), or the intermediate-spin (IS) state ($t_{2g}^5e_g^1$, $S = 1$), because the crystal-field splitting strength is slightly larger than the Hund's rule coupling energy and the small energy difference ($\approx$0.03 eV) allows thermal excitation of t_{2g} electrons into the e_g energy level [5, 11, 12]. In the range of 110–350 K, the ratio of HS to LS Co ions stabilizes near 50:50, and above 350 K the remaining LS Co^{III} are progressively converted into the HS state. Upon doping divalent Sr^{2+} into $LaCoO_3$, some of trivalent Co ions are transformed into tetravalent Co which also contain a mixture of low and high spin sates (HS: Co^{4+}, $t_{2g}^3e_g^2$, $S = 5/2$ [13]; LS: Co^{IV}, $t_{2g}^5e_g^0$, $S = 1/2$ [5]; IS: Co^{iv}, $t_{2g}^4e_g^1$, $S = 3/2$ [14]). Additionally, tetravalent Co can stabilize HS Co^{3+} near it down to the lowest temperature [5]. Besides, a physical or chemical pressure can be another possible factor controlling the spin state of cobalt oxides [15–17]. This spin-state transition is an interesting subject.

The magnetic phase diagram of $La_{1-x}Sr_xCoO_3$ has been established by different investigators [5, 6, 18]. The diagram clearly shows that a ferromagnetic (FM) transition appears at $x > 0.2$–0.25 with increasing Sr content. However, it is not a long-range ferromagnetic order. The magnetization measurement result indicates a cluster-glass behaviour for the $La_{1-x}Sr_xCoO_3$ system at $x > 0.18$, because those domains with rich Co^{4+} ions stabilizing the nearby HS Co^{3+} form many ferromagnetic clusters in the LS Co^{III} matrix [18]. When the Sr content is over 0.25, the conductivity displays a ferromagnetic metallic behaviour while it is insulator-like below 0.2.

Since the spin states of Co ions play such an important role and they can be thermally excited and modified by tetravalent Co due to Sr doping or chemical pressure, it is of interest to try the substitution of magnetic ions for the A-site, which has seldom been done in this system. In our present work, we doped magnetic Gd^{3+} ions with a magnetic moment $\mu_{\text{eff}} \approx 8.0\,\mu_B$ into $La_{0.67}Sr_{0.33}CoO_3$ cobaltites in order to investigate the coupling of A-site ions and Co ions. The radius difference between Gd^{3+} and La^{3+} is relatively large (Gd^{3+}: 1.107 Å; La^{3+}: 1.216 Å) [19]. We calculated the tolerance factor t and found it is in the range of 0.923–0.972 for Gd-doped $La_{0.67}Sr_{0.33}CoO_3$. These t-values are appropriate for the perovskite structure. In fact, we have a series of doping level samples up to $Gd_{0.67}Sr_{0.33}CoO_3$ associated with some structural changes in the high-doping ones. In addition, we prepared Gd-doped $La_{0.7-x}Gd_xSr_{0.3}MnO_3$ as a comparison, and found that the magnetic behaviour is totally different from the Gd-doped Co-based oxides.

2. Experimental details

Polycrystalline samples $La_{0.67-x}Gd_xSr_{0.33}CoO_3$ ($x = 0.00, 0.05, 0.10, 0.20, 0.30, 0.40, 0.50, 0.60, 0.67$) were synthesized by a conventional solid state reaction method. Appropriate amounts of La_2O_3 (preheated at 400 °C for 4 h before measurement), Gd_2O_3, $SrCO_3$ and

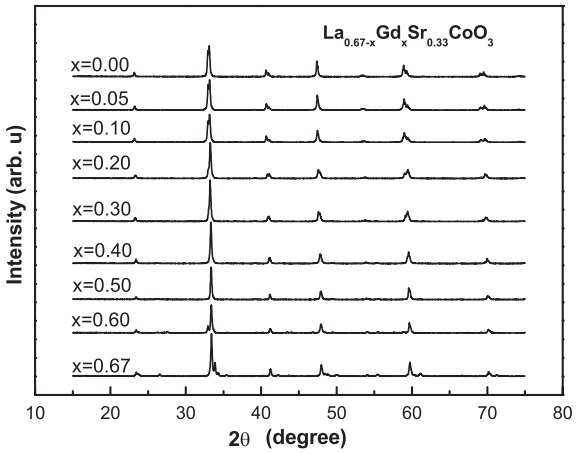

Figure 1. X-ray-diffraction patterns of $La_{0.67-x}Gd_xSr_{0.33}CoO_3$ ($0 \leqslant x \leqslant 0.67$).

Co_2O_3, were mixed and heated in air at 800 °C for 14 h, 1000 °C for 12 h, and 1200 °C for 24 h with intermediate grinding. Finally, the powder was pressed into pellets and sintered in air at 1300 °C for 30 h, then furnace cooled down to room temperature. (When preparing the sample $x = 0.67$ at 1300 °C, the pellets of $Gd_{0.67}Sr_{0.33}CoO_3$ melted. Then it was prepared again at 1200 °C as the final sintering temperature.) To make a comparison, we prepared $La_{0.7-x}Gd_xSr_{0.3}MnO_3$ ($x = 0.40, 0.60$) by the same method.

The structure and phase purity of all as-prepared samples were checked by powder x-ray diffraction (XRD) using Cu Kα radiation at room temperature. As shown in figure 1, the XRD patterns of $La_{0.67-x}Gd_xSr_{0.33}CoO_3$ prove the single phase of these samples (except for $x = 0.60$ and 0.67 which contain a very little impurity) and a rhombic to orthorhombic structure transition upon increasing the Gd content up to $x = 0.40$. The measurements of magnetization were carried out using a Lake-Shore 9300 vibrating sample magnetometer (VSM). The resistance was measured by standard a four-probe method in the temperature range 4.2–300 K with an Oxford 15T system.

3. Results and discussions

3.1. Magnetism

After zero-field cooling (ZFC) down to 5 K, the magnetization data were collected in a 100 Oe magnetic field during the warming process. In figure 2, it can be seen that Gd doping not only drives the Curie temperature (T_C) to lower temperature but also weakens the magnetization of the system. The values of T_C for all samples, defined as the inflection point in the M–T curves, are summarized in table 1. In figure 5 we plot T_C versus the t-factor. It is apparent that with decreasing t-factor (increasing Gd content) T_C is greatly reduced. Amazingly, for the samples with $x > 0.10$, their magnetization increases rapidly below 60 K with cooling, whereas in all of the reported CMR materials, M usually decreases or tends toward saturation with the temperature decreasing below T_C. For an example, the magnetization decreases with cooling in Gd-doped manganites $La_{2/3-x}Gd_xCa_{1/3}MnO_3$ or $La_{2/3-x}Gd_xSr_{1/3}MnO_3$, which has been assigned to spin-canted, even antiferromagnetic or ferrimagnetic behaviour [20–23]. To have a direct comparison, we show the magnetization of $La_{0.7-x}Gd_xSr_{0.3}MnO_3$ ($x = 0.40$ and 0.60) in figure 3. For $x = 0.40$, M decreases below 40 K, and for $x = 0.60$ it sharply drops to zero

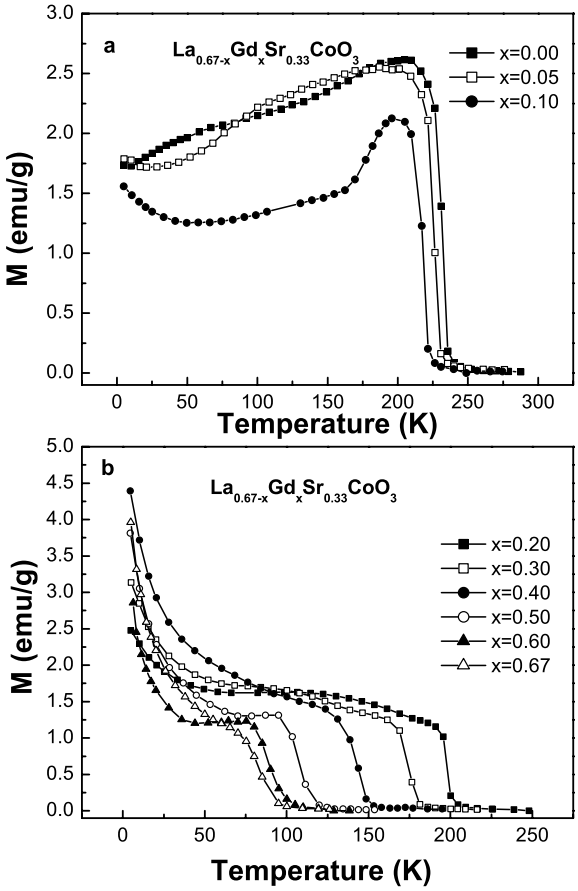

Figure 2. The temperature dependence of magnetization for $La_{0.67-x}Gd_xSr_{0.33}CoO_3$ samples in a 100 Oe magnetic field.

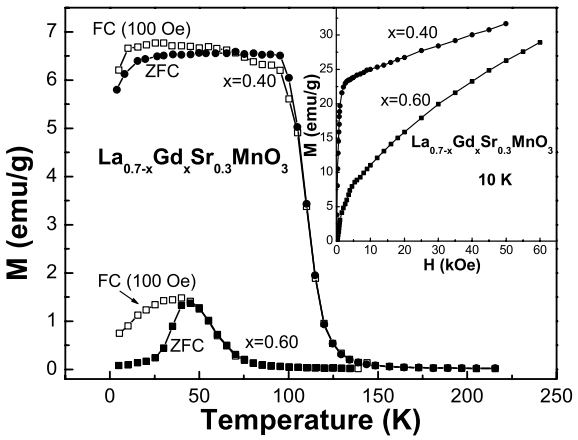

Figure 3. The temperature dependence of magnetization for $La_{0.7-x}Gd_xSr_{0.3}MnO_3$ ($x = 0.40$, 0.60) samples; the insets shows M–H curves at 10 K.

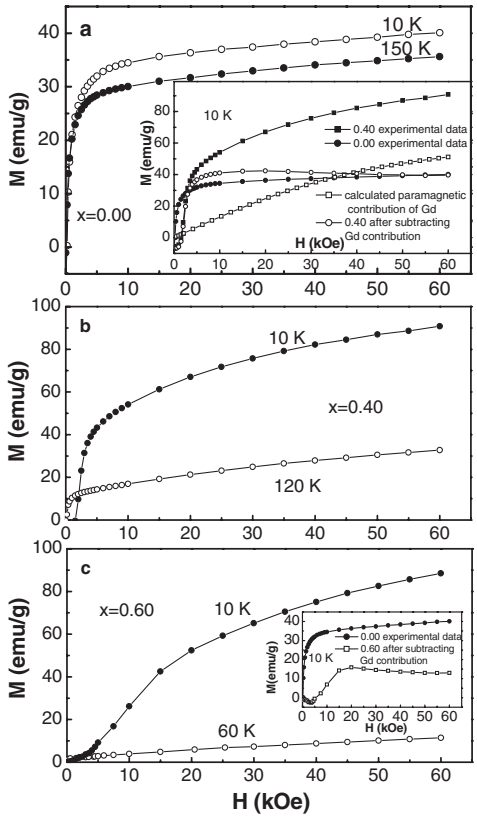

Figure 4. The field dependence of magnetization for $La_{0.67-x}Gd_xSr_{0.33}CoO_3$ ($x = 0.00$, 0.40, 0.60) samples. The insets in (a) and (c) show the Gd^{3+} contribution to the magnetization for $x = 0.40$ and 0.60.

at low temperature. Even after a field-cooling process, the M–T curve cannot recover its flat shape below T_C. In the inset of figure 3, the magnetization does not even reach saturation under 60 kOe, especially for the sample with $x = 0.60$. All of these features clearly demonstrate that antiferromagnetism occurs with Gd doping in manganite $La_{0.7}Sr_{0.3}MnO_3$. Some investigators have suggested that the Gd sublattice being antiparallel to the Mn sublattice contributes to this antiferromagnetism [21, 22]. In our samples, a totally different result from the Mn-based oxide is observed in figure 2. In contrast, we can conclude that a parallel alignment of Gd and Co magnetic moments may be a reasonable arrangement. However, the problem is whether this alignment is forced by field/temperature or is a spontaneous behaviour; namely, is it due to paramagnetism (PM) or ferromagnetism? In fact, a similar experimental result in which a significant increase of magnetization occurs at low temperature under 10.85 and 50 kOe fields has been reported in $Gd_{0.5}Ba_{0.5}CoO_3$ by Troyanchuk *et al* [24], and they indicated that it could be ascribed to the paramagnetic contribution of a Gd sublattice, yet their focus is not on this point. The following experimental results and analysis will elucidate this to some extent.

To get a clearer picture of the magnetic behaviour, we measured the field (H) dependence of the magnetization (M) at some temperature points for three typical samples (shown in figure 4). The two M–H curves for every sample are measured at two special temperature points. One of the curves is measured at 10 K, that is in the rising region of the magnetization

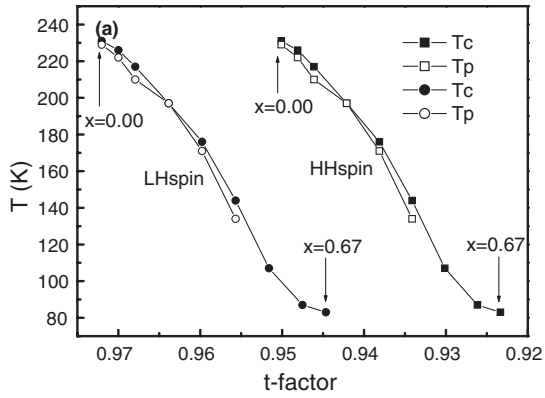

Figure 5. t-factor versus T_C and T_p when trivalent Co is in the LS and the HS state, respectively. 'LHspin' curves represent the results calculated with LS trivalent and HS tetravalent Co radii, and 'HHspin' curves represent the results calculated using HS trivalent and HS tetravalent Co radii. We calculated two curves for the two extreme situations because we are not sure how many trivalent Co ions are in the LS state.

Table 1. The measured Curie temperature T_C, transition temperature T_p of resistivity, and fitting parameters ρ_0, ρ_2, which are described in text.

Sample (x)	0.00	0.05	0.10	0.20	0.30	0.40	0.50	0.60	0.67
T_C (K)	231	226	217	197	176	144	107	87	83
T_p (K)	229	222	210	197	171	134	—	—	—
ρ_0 (0 T) (10^{-6} Ω cm)	52.70	62.13	83.39	125.42	121.77				
ρ_2 (0 T) (10^{-9} Ω cm)	2.010	1.993	1.838	2.574	1.597				
ρ_0 (6 T) (10^{-6} Ω cm)	53.83		84.07	127.37	120.34				
ρ_0 (6 T) (10^{-9} Ω cm)	1.370		1.325	2.087	1.522				

(below 60 K), and the other is in the temperature between 60 K and T_C. The M–H curves of $x = 0.00$ in figure 4(a) show a ferromagnetic shape well at both 10 K and 150 K. However, the M–H curves at 10 K for $x = 0.40$ and 0.60 in figures 4(b) and (c) are quite different from that in figure 4(a) for $x = 0.00$, and their M increases consistently with applied field, without saturation, and, with increasing Gd content, rises more rapidly. This is similar to the results of the $La_{0.7-x}Gd_xSr_{0.3}MnO_3$ system (the inset of figure 3). However, the M–T curves of $La_{0.7-x}Gd_xSr_{0.3}MnO_3$ (figure 3) and $La_{0.67-x}Gd_xSr_{0.33}CoO_3$ (figure 2) are noticeably different from each other. As we know, if the ferromagnetic coupling works, the magnetization should be saturated in such a high field, while this is not the case, and with more Gd the magnetization process is broadened. So, the probability of ferromagnetic coupling between the Gd sublattice and the Co sublattice can be excluded.

The magnetism measurement gives many interesting results. We now present the following scenario to analyse these results. Upon Gd doping, the effects caused directly by Gd are: (1) the lattice parameters are changed, (2) the internal magnetic environment of the Co ions is modified. The radius of Gd^{3+} is smaller than La^{3+}. Using Gd to substitute La leads to the reduction of the average radius of the A-site, producing a distortion of the Co–O–Co bond, such as a decrease of the Co–O–Co angle [9, 14], which weakens the coupling among the Co ions. This is manifested by the fact that T_C is driven to a lower temperature and the magnetization exhibits a drop with Gd doping. On the other hand, Gd^{3+} has a rather big effective magnetic moment. This disordered magnetic potential acts on Co–O–Co, resulting in the blocking of the

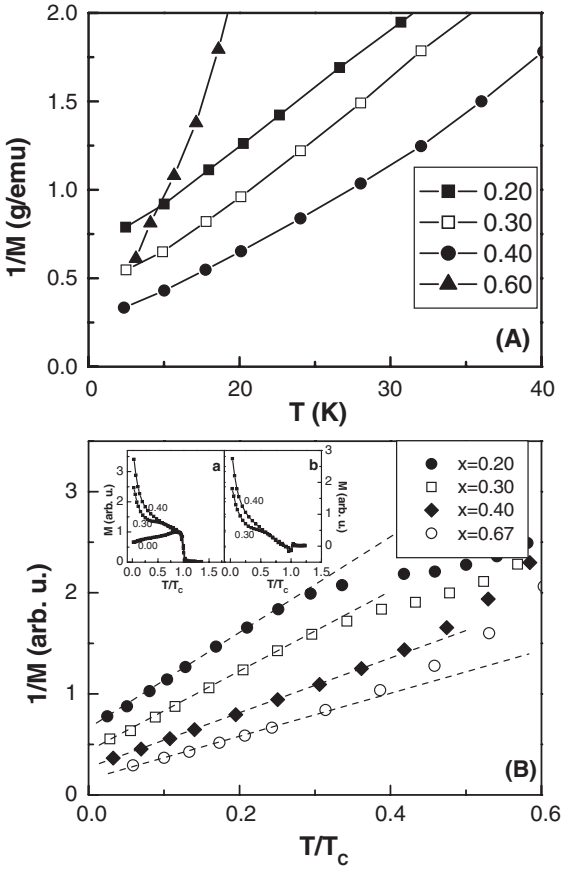

Figure 6. $1/M$ versus T/T_C. (A) using treatment 1; (B) using treatment 2 (see the text). The dashed line is a guide to the eye. Inset (a) shows the normalized M–T curves near T_C and the M value at $0.9T_C$. Inset (b) shows the M–T curves after subtracting the $x = 0.00$ curve.

long-range ferromagnetic order in Co–O–Co. This may be another reason for T_C decreasing with increasing Gd content.

Fgure 2(b) clearly shows the great reduction of T_C with increasing x (see table 1), while the starting temperature for significant increase of M does not change a lot; it is approximately between 60 and 40 K for $0.20 \leqslant x \leqslant 0.67$. To assure the origin of the magnetization increase at low temperature, we apply the following treatment to the M–T data at low field. First, the FM matrix component of the magnetization by the Co sublattice is subtracted from the M–T curves based on the platform M-value after the PM–FM transition. Then the $1/M$ versus T curve below 60 K is plotted in figure 6(A). However, the linearity is not ideal. We believe that this is because the method that we use to treat the M–T curves is imperfect. Since the M–T curves of the $x = 0.00$, 0.10, 0.05 samples drop down gradually at low temperature, it is reasonable that the ones of the other samples would drop down, too, if they are without the contribution of Gd paramagnetism at low temperature. Therefore, the treatment above ignored the Co sublattice's behaviour at low temperature. Therefore we found a new treatment which would solve this problem. We follow these steps. First, the M–T curves in figure 2(b) are normalized by the T_C and M value at $0.9T_C$ (scaled as T/T_C, the rising region of M is approximately

below 0.30, 0.35, 0.40 and 0.5 T_C for $x = 0.20$, 0.30, 0.40, and 0.67, respectively); then, the M–T curve at $x = 0.00$ is subtracted from the others; finally, the subtracted M–T curves are replotted as $1/M$ versus T. Figure 6(B) show the results for $x = 0.20$, 0.30, 0.40 and 0.67. The inset (a) gives the normalized curves, and the inset (b) shows the subtracted curves, which is the contribution of Gd sublattice. This treatment, although it is still an approximate one, seems to be more reasonable since the reduction of the Co sublattice magnetism induced by Gd doping can be largely excluded through the method of normalization, and the similar Co sublattice behaviour can also be removed from various doping-level samples. In fact, it can be seen in figure 6(B) that the $1/M$–T curves clearly demonstrate a linear relation below 0.3–0.5T_C. This follows the Curie–Weiss law, which describes the paramagnetic behaviour at low field. However, there is one notable thing from figure 6(B): the negative interception at temperature axis. In our system, the Gd paramagnetism parasitizes in the FM matrix which is attributed to the ferromagnetic arrangement of Co–O–Co. Therefore, we can deduce that there may exist a rather weak coupling between the Gd and Co sublattices; that is to say, the ferromagnetism of the Co sublattice causes ferromagnetic fluctuations in the Gd sublattice. These FM fluctuations are antiferromagnetically arranged with the FM Co sublattice. As a result, the system magnetization after subtracting the FM matrix will show an antiferromagnetic characteristic. However, it is also possible that the impreciseness of this subtraction method causes the upward translation for the line.

At high field, through the standard Brillouin function expression in a paramagnetic system,

$$\langle \mu \rangle = J g_J \mu_B B_J(x)$$

where $B_J(x) = (1 + 1/2J)\coth[(1 + 1/2J)x] - (1/2J)\coth(x/2J)$ is the Brillouin function, $x = Jg_J\mu_B B/k_B T$, we calculated the field dependence of the Gd paramagnetic magnetization at 10 K per gram of sample (shown in the inset of figure 4(a)). Then, we subtracted the Gd paramagnetic contribution from the experimental M–H curve of $x = 0.40$ at 10 K. The subtracted M–H curve is plotted in the inset. It is very similar to the one of undoped sample $x = 0.00$, which implies that the rapid increase of magnetization at low temperature (<60 K) is indeed derived from the Gd paramagnetic contribution. However, we find the subtracted result for $x = 0.60$ is very different from the undoped sample. It is much smaller than the M–H values of $x = 0.00$ at 10 K (the inset of figure 4(c)). From the features of M–H curve, it seems that there are some AFM or ferrimagnetism fractions contributing to the lack of saturation for heavily-doped samples. Of course, this AFM or ferrimagnetism should come from Co–O–Co since lattice distortions can cause a change of exchange interaction.

The substitution of Gd for La causes an essentially different result in the manganites and cobaltites. In the introduction, we mentioned that the primary divergence between Co and Mn ions is the electronic structure and spin state. Mn^{3+}/Mn^{4+} has a half-filled t_{2g} state which forms a strong localized core spin. Therefore, Mn^{3+}/Mn^{4+} can magnetically couple with Gd^{3+}. In other words, after transition the FM Mn^{3+}–O–Mn^{4+} induces the ferromagnetism of the Gd sublattice, and both magnetic lattices antiferromagnetically couple with each other, which leads to the lowest energy of the system. The trivalent Co ion does not own a half-filled t_{2g} state, and, especially, it has an LS state with zero spin. In the $La_{0.67}Sr_{0.33}CoO_3$ system many of trivalent Co ions are in the LS state, so that the coupling between the Gd and Co sublattices will be rather weak. The FM Co^{3+}–O–Co^{4+} cannot cause the parallel arrangement of Gd^{3+} magnetic moments, so the Gd sublattice remains in the PM state. The macromagnetism of the system is the contribution of the FM Co sublattice added to the PM Gd sublattice. In summary, the reason for the completely different magnetic behaviour, AFM in Gd-doped cobaltites, and PM in Gd-doped manganites, is that the magnetism of Mn–O–Mn is stronger while that of Co–O–Co is weaker.

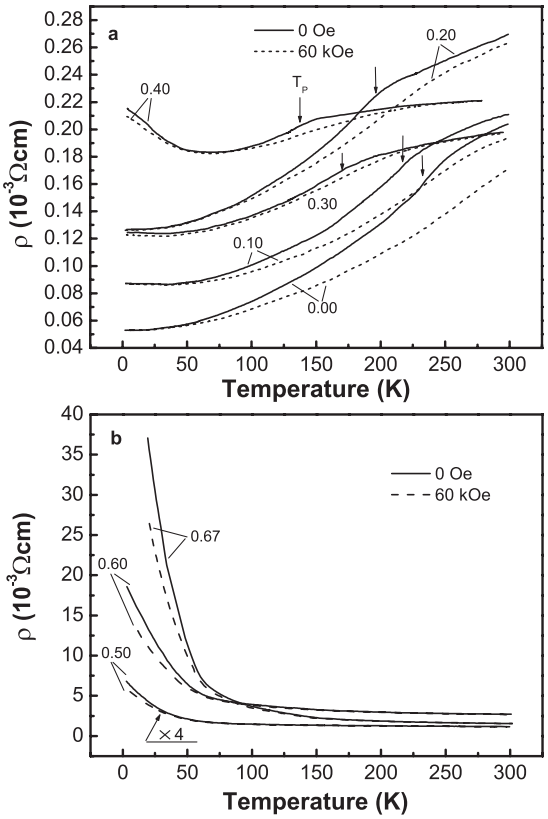

Figure 7. The temperature dependence of the resistivity for $La_{0.67-x}Gd_xSr_{0.33}CoO_3$ ($0 \leqslant x \leqslant 0.67$) samples under zero and 60 kOe magnetic field (arrows show the position of T_p): (a) low-doped samples, (b) high-doped samples.

3.2. Electrical resistivity

The temperature dependence of the resistivity under zero and 60 kOe field is shown in figure 7. The conductive behaviour for $La_{0.67}Sr_{0.33}CoO_3$ is similar to that of a conventional ferromagnet metal, which is consistent with the previous reports [5, 10]. In figure 7(a), it is clear that there is a steep change in the slope of the ρ–T curve at T_p for low-doped samples. The transition temperatures T_p (defined as the peak of $d\rho/dT$) are summarized in table 1, and they are approximately equal to T_C, which implies a correlation between the conductive and magnetic transition. When $T > T_p$, the metallic conductivity is in the PM background; when $T < T_p$ it is in the FM state. As x increases, the sample's resistivity rises gradually. However, the sample $x = 0.20$ is abnormal, since its resistivity is larger than the one of the sample $x = 0.30$. A similar occurrence appeared in the literature for $La_{0.8}Sr_{0.2}CoO_3$, which is in the sensitive composition region [7, 25]. Here, it is different, and the reason is unclear. For $x > 0.40$ in figure 7(b), the system exhibits a semiconducting behaviour ($d\rho/dT < 0$). For $x = 0.40$ in figure 7(a), the conductivity shows metallic behaviour ($d\rho/dT > 0$) at high temperature; when the temperature decreases, a slope change appears, which is the same as for samples $x < 0.40$; with further decreasing temperature, the resistivity increases and semiconducting behaviour occurs. Therefore, $x = 0.40$ is a critical doping point. Sun *et al* [26] found the same result in $La_{0.67}Sr_{0.33}CoO_3$ with Fe doping. Upon Fe doping, some of Co are replaced by Fe, and it

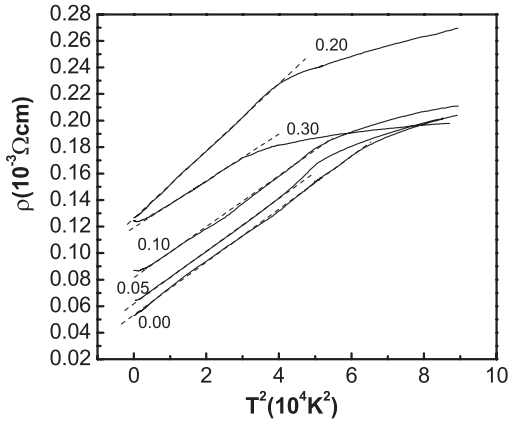

Figure 8. Resistivity in zero field fits to ρ–T^2 ($0 \leqslant x \leqslant 0.30$). The dashed lines are guides to the eye.

is considered that the blocking of some of the transport channels results in the enhancement of resistivity. Here in $La_{0.67-x}Gd_xSr_{0.33}CoO_3$, the Gd doping does not block the Co–O–Co transport channel directly, and the quantity or proportion of tetravalent and trivalent Co ions is not modified, as it is an A-site substitution. The probable reasons for the increase of resistivity and the metal–semiconductor transition are the following.

(1) The radius of the Gd^{3+} ion is smaller than that of La^{3+}. The Gd substitution for La reduces the average radius of A-site, leading to changes of the Co–O bond length and Co–O–Co angle, weakening the ferromagnetic coupling of Co–O–Co and forming an energy gap that is against carrier transfer between Co–O–Co.
(2) The disordered local magnetic and Coulumb potential from Gd^{3+} ions give a strong scattering on the carriers. As a result, the conductivity is reduced smoothly, and semiconducting behaviour appears at high-doping level.

In Gd-doped manganites, the appearance of antiferromagnetism immediately induces the increases of resistivity and insulating behaviour at low temperature. However, there is no obvious correlation between the increase of magnetization and the IM transition with doping in $La_{0.67-x}Gd_xSr_{0.33}CoO_3$. This result simply indicates the weak coupling between Gd^{3+} and Co ions, too. To analyse the conductive behaviour in detail, we fitted the resistivity to an expression of the form $\rho = \rho_0 + \rho_2 T^2$ for metallic samples, as a significant T^2 dependence of resistivity [27] is often observed in metallic ferromagnets such as Fe, Co, and Ni. The first term ρ_0 is temperature independent; it arises from the contribution of grain or domain boundaries, and defects because of polycrystalline samples. In figure 8 the relations of ρ versus T^2 are plotted. A nearly perfect linearity for all curves is demonstrated extending to almost the full range of the region below T_C, except for a small deviation at very low temperature. The origin of the T^2 term has been discussed in detail by Snyder *et al* [28]. They suggested a single-particle, spin-flip excitation mechanism for the T^2 dependence. Although a general electron–electron scattering mechanism also gives a T^2 dependence of the resistivity which is not necessarily field dependent, this is effective at low temperature because the T^2 law can dominate only when the thermal vibration of the lattice has been suppressed. We fitted the resistivity data under 60 kOe field to the above expression. It is found that the range of T^2 dependence still extends to nearly T_C, and the coefficient of the T^2 term decreases greatly. Meanwhile, the temperature-independent term ρ_0 increases a little. The parameters ρ_0, ρ_2 are

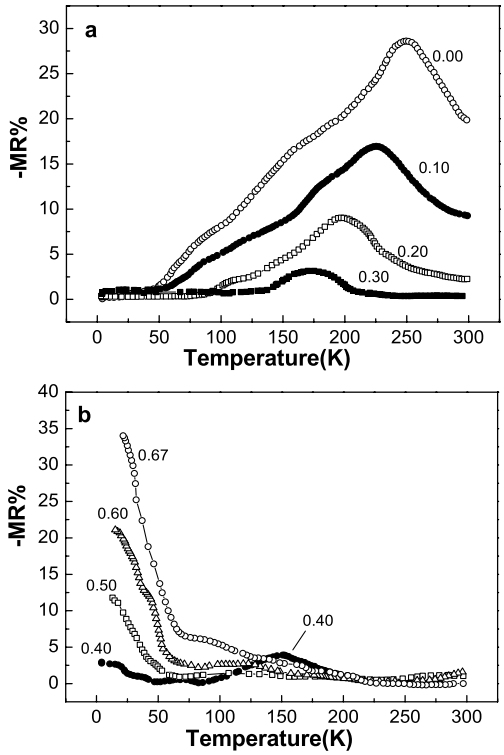

Figure 9. The temperature dependence of the magnetoresistance for $La_{0.67-x}Gd_xSr_{0.33}CoO_3$ samples: (a) low-doped samples; (b) high-doped samples.

summarized in table 1. This may indicate that the spin-flip excitation mechanism is suitable in our system.

3.3. Magnetoresistance

In figure 7 we show the temperature dependence of the resistivity under zero and 60 kOe magnetic field, respectively. Under applied magnetic field, the resistivity of $La_{0.67-x}Gd_xSr_{0.33}CoO_3$ is compressed in most of the temperature range, though the extent of the change is not so great as in mixed-valence manganites. The MR, defined as $(\rho(H) - \rho(0))/\rho(H)$, is plotted in figure 9. For the metallic samples $x = 0.00, 0.10, 0.20$ and 0.30, the MR shows a peak near T_C, and this occurs in a large temperature range, which is the same as the usual CMR and can be attributed to the strongest suppression of spin-disordering with application of the magnetic field. With Gd doping, the MR peak is gradually reduced, and the MR range is narrowed. Meanwhile, the low-temperature MR is enhanced. When $x = 0.40$, the low-temperature MR is obviously comparable with the peak one at T_C. For the high-doping level samples $x = 0.50$, 0.60, and 0.67, the MR keeps increasing at low temperature and the MR peaks disappear near T_C, which indicates that the mechanism of low-temperature MR should be different from that of the high-temperature MR near T_C. It could be correlated to the grain boundary effects or other sources of spin disorder and frustration associated with the weakening of the ferromagnetism of Co–O–Co, such as the suppression of disordered local magnetic moments of Gd, which leads to the reduction of magnetic scattering. Interestingly,

the MR in $La_{0.67-x}Gd_xSr_{0.33}CoO_3$ is rather different from that in $La_{0.7-x}Gd_xSr_{0.3}MnO_3$, since Gd doping in $La_{0.7}Sr_{0.3}MnO_3$ enormously enhances the MR near T_C [22]. Because of the complex magnetic structure and spin configuration in cobaltites, the mechanism of CMR is not yet well understood, and deserves more detailed attention.

4. Conclusion

In summary, we report some experimental results in $La_{0.67-x}Gd_xSr_{0.33}CoO_3$, which is very different from the $La_{0.7-x}Gd_xSr_{0.3}MnO_3$ system due to the divergence of the electronic structure and spin state between Mn and Co. The magnetization of this system reveals a surprising behaviour that the magnetization rises rapidly below 60 K with the decreasing temperature. This can be well understood in terms of the paramagnetism of the Gd sublattice. This implies that the coupling between the Gd and Co sublattices is weak and negligible. With the incorporation of Gd, T_C shifts from 231 K for $x = 0.00$ to 83 K for $x = 0.67$. Resistivity results display a good T^2 relation for metallic samples. The MR peak occurs at T_C for $0 \leqslant x \leqslant 0.40$. Then it disappears, while the low-temperature MR is large for $0.40 < x \leqslant 0.67$.

Acknowledgments

The authors would like to thank Yanan Bao, Dr Young Sun and Deliang Zhu for help in experiments. This work was supported by the National Nature Science Foundation of China (No. 19934003) and the State Key Project of Fundamental Research, China (001CB610604).

References

[1] Von Helmolt R, Wecker J, Holzapfel B, Schultz L and Samwer K 1993 *Phys. Rev. Lett.* **71** 2331
[2] Goodenough J B *et al* 1999 *Aust. J. Phys.* **52** (2)
A discussion organized by Blamire M, Cohen L F, Edwards D M and Macmanhs-Driscoll J L (ed) 1998 *Phil. Trans. R. Soc.* A **356** 1469–792
Ramirez A P 1997 *J. Phys.: Condens. Matter* **9** 8171
Dagotto E, Hotto T and Moreo A 2001 *Phys. Rep.* **344** 1–153
Coey J M D, Viret M and Von Molnár S 1999 *Adv. Phys.* **48** 167
[3] Zener C 1951 *Phys. Rev.* **82** 403
Millis A J, Littlewood P B and Shraiman B I 1995 *Phys. Rev. Lett.* **74** 5144
Hwang H Y, Cheong S-W, Radaelli P G, Marezio M and Batlogg B 1995 *Phys. Rev. Lett.* **75** 914
Millis A J, Shraiman B I and Mueller R 1996 *Phys. Rev. Lett.* **77** 175
[4] Briceño G, Chang H, Sun X D, Schultz P G and Xiang X D 1995 *Science* **270** 273
[5] Señarís-Rodríguez M A and Goodenough J B 1995 *J. Solid State Chem.* **118** 323
[6] Mahendiran R and Raychaudhuri A K 1996 *Phys. Rev.* B **54** 16044
[7] Golovanov V, Mihaly L and Moodenbaugh A P 1996 *Phys. Rev.* B **53** 8207
[8] Mahendiran R, Raychaudhuri A K, Chainani A and Sarma D D 1995 *J. Phys.: Condens. Matter* **7** L561
[9] Caciuffo R, Rinaldi D, Barucca G, Mira J, Rivas J, Señarís-Rodríguez M A, Radaelli P G, Fiorani D and Goodenough J B 1999 *Phys. Rev.* B **59** 1068
[10] Yamaguchi S, Taniguchi H, Takagi H, Arima T and Tokura Y 1995 *J. Phys. Soc. Japan* **64** 1885
[11] Raccah P M and Goodenough J B 1967 *Phys. Rev.* B **155** 932
[12] Asai K, Gehring P, Chou H and Shirane G 1989 *Phys. Rev.* B **40** 10982
[13] Chainani A, Mathew M and Sarma D D 1992 *Phys. Rev.* B **46** 9976
[14] Potze R H, Sawatzky G A and Abbate M 1995 *Phys. Rev.* B **51** 11501
[15] Chenavas J, Joubert J C and Hagenmuller P 1971 *J. Phys. Chem. Solids* **32** 407
[16] Sun J R, Li R W and Shen B G 2001 *J. Appl. Phys.* **89** 1331
[17] Sun J R and Wong H K 1999 *Appl. Phys. Lett.* **75** 1772
[18] Itoh M, Natori I, Kubota S and Motoya K 1994 *J. Phys. Soc. Japan* **63** 1486

[19] Shannon R D 1976 *Acta Crystallogr.* A **32** 751
[20] Guo Z B, Huang H, Ding W P and Du Y W 1997 *Phys. Rev.* B **56** 10789
[21] Snyder G J, Booth C H, Bridges F, Hiskes R, DiCarolis S, Beasley M R and Geballe T H 1997 *Phys. Rev.* B **55** 6453
[22] Sun Y, Salamon M B, Tong W and Zhang Y H 2002 *Phys. Rev.* B **66** 094414
[23] Rubinstein M, Gillespie D J, Snyder J E and Tritt T M 1997 *Phys. Rev.* B **56** 5412
[24] Troyanchuk I O, Kasper N V and Khalyavin D D 1998 *Phys. Rev. Lett.* **80** 3380
[25] Ganguly P, Anil Kumar P S, Santhosh P N and Mulla I S 1994 *J. Phys.: Condens. Matter* **6** 533
[26] Sun Y, Xu X J and Zhang Y H 2000 *Phys. Rev.* B **62** 5289
[27] Mannari I 1959 *Prog. Theor.* **22** 335
[28] Snyder G J, Hiskes R, DiCarolis S, Beasley M R and Geballe T H 1996 *Phys. Rev.* B **53** 14434